Biophysical Journal Volume 82 February 2002 929–943 

# History-Dependent Mechanical Properties of Permeabilized Rat Soleus Muscle Fibers

Kenneth S. Campbell and Richard L. Moss
Department of Physiology, University of Wisconsin–Madison, Wisconsin 53706 USA

ABSTRACT Permeabilized rat soleus muscle fibers were subjected to repeated triangular length changes (paired ramp stretches/releases, 0.03 $l_0$, ± 0.1 $l_0$ $s^{-1}$ imposed under sarcomere length control) to investigate whether the rate of stiffness recovery after movement increased with the level of $Ca^{2+}$ activation. Actively contracting fibers exhibited a characteristic tension response to stretch: tension rose sharply during the initial phase of the movement before dropping slightly to a plateau, which was maintained during the remainder of the stretch. When the fibers were stretched twice, the initial phase of the response was reduced by an amount that depended on both the level of $Ca^{2+}$ activation and the elapsed time since the first movement. Detailed analysis revealed three new and important findings. 1) The rates of stiffness and tension recovery and 2) the relative height of the tension plateau each increased with the level of $Ca^{2+}$ activation. 3) The tension plateau developed more quickly during the second stretch at high free $Ca^{2+}$ concentrations than at low. These findings are consistent with a cross-bridge mechanism but suggest that the rate of the force-generating power-stroke increases with the intracellular $Ca^{2+}$ concentration and cross-bridge strain.

## INTRODUCTION

Skeletal muscles are stiff for small movements. When they are stretched, tension rises sharply during the first few nanometers half-sarcomere$^{-1}$ of the imposed movement and less sharply thereafter. This nonlinear mechanical behavior is characteristic of both relaxed (Hill, 1968) and actively contracting muscle fibers (Edman et al., 1978; Flitney and Hirst, 1978; Lombardi and Piazzesi, 1990; Stienen et al., 1992; Getz et al., 1998; Edman, 1999) and has been attributed to the stretch and subsequent cyclic reattachment of cross-bridges linking the actin and myosin filaments.

The nonlinear properties of muscles depend on their history of movement. If, for example, a muscle is stretched twice, the initial phase of the second stretch response depends on the time interval between the stretches. When the two stretches follow closely one after the other, the initial stiffness of the second stretch response is reduced; when the stretches are separated by a relatively long time period, the two responses appear identical. Muscles therefore possess a time-dependent short-range elasticity that resets after movement.

This history-dependent behavior, first described for relaxed muscles by Denny-Brown in 1929, is attributed to a thixotropic effect (Campbell and Lakie, 1998; Campbell and Moss, 2000). No clear consensus on the underlying mechanism has yet been established, although several possible theories have been proposed (for review, see Proske and Morgan, 1999). For example, Mutungi and Ranatunga (2000) suggested that the history-dependent behavior could reflect changes in the mechanical properties of titin filaments after an imposed stretch. This conjecture was strengthened when Kellermayer et al. (2001) and Minajeva et al. (2001) reported that the stiffness of titin filaments can be reduced by large movements, but there is still some doubt as to whether titin filaments can underlie the biphasic tension response observed in resting muscles (see Discussion in Campbell and Lakie, 1998).

Although Mutungi and Ranatunga's hypothesis remains a genuine possibility for relaxed muscles, it seems to us that the main problem with attributing the history dependence of the mechanical properties to titin filaments (or other passive viscoelastic structures) is that these mechanisms do not seem to be able to account for the thixotropic properties observed in contracting muscles. In a recent paper (Campbell and Moss, 2000) we measured the response of permeabilized rabbit psoas fibers subjected to repeated triangular length changes (paired ramp stretches and releases). The stiffness of the second stretch response was reduced at every activating $Ca^{2+}$ concentration, and the magnitude of the reduction scaled in a similar manner to the developed tension as the level of $Ca^{2+}$ activation was raised from negligible to saturating values.

These findings suggest that history dependence is inherent to the contractile apparatus itself and we therefore proposed that the decrease in stiffness that we observed in contracting muscles reflected a temporary reduction in the number of cross-bridges attached between the thick and thin filaments. If we were to have attributed the history dependence of the muscle's stiffness to titin filaments or other passive components, the resistance of these structures to movement would have had to scale with the level of active force generation, a situation that we believe is unlikely.

A similar cross-bridge mechanism had already been proposed for relaxed muscles. In 1968, Hill suggested that the biphasic tension response measured in whole amphibian

*Submitted June 21, 2001, and accepted for publication November 2, 2001.*
Address reprint requests to Kenneth S. Campbell, Department of Physiology, 127 SMI, 1300 University Avenue, Madison, WI 53706. Tel.: 608-262-7586; Fax: 608-265-5512; E-mail: campbell@physiology.wisc.edu.

0006-3495/02/02/929/15 $2.00

muscles represented the stretch and subsequent "frictional resistance" of a very small number of cross-bridges, which continued to cycle through the normal kinetic scheme under resting conditions. Herbst (1976) later developed this hypothesis and proposed that the history dependence of the biphasic response (which Hill did not specifically investigate) could be explained by long-lived changes in the number of attached cross-bridges after movement. This "cross-bridge theory" has been supported by a number of other workers (Lakie and Robson, 1990; Campbell and Lakie, 1998; Proske and Morgan, 1999) but remains controversial (Mutungi and Ranatunga, 2000).

Although it is possible that the thixotropic properties observed in relaxed and contracting muscles reflect two quite distinct mechanisms, Occam's razor favors the general cross-bridge hypothesis because it can account, at least qualitatively, for the history-dependent behavior observed at different levels of $Ca^{2+}$ activation. Another advantage of the theory is that it provides a possible explanation for an important quantitative difference between the thixotropic properties of relaxed and contracting fibers, the rate of stiffness recovery.

In the cross-bridge hypothesis, this recovery rate reflects the speed at which the cross-bridge populations redevelop after movement. It is therefore related to the overall rate of cross-bridge turnover, a parameter that is thought to be $Ca^{2+}$ dependent because measured values of $k_{tr}$, the rate of tension development after a period of unloaded shortening, increase when the free $Ca^{2+}$ concentration is raised from minimum to saturating values (Brenner, 1988; for review, see Gordon et al., 2000). All other things being equal, the cross-bridge hypothesis therefore suggests that the rate of stiffness recovery will increase with the level of $Ca^{2+}$ activation. Verification of this conjecture would provide strong support for the theory.

In our previous experiments (Campbell and Moss, 2000), we found that stiffness recovered substantially faster ($\sim$1 $s^{-1}$, 15°C) in contracting rabbit psoas fibers than in relaxed intact frog fibers (0.1 $s^{-1}$ or less, 5°C; Lännergren, 1971; Campbell and Lakie, 1998), but we were unable to measure the $Ca^{2+}$ dependence of the recovery rate. The striation pattern in the psoas fibers deteriorated irreversibly after 20 to 30 stretches, and we were therefore unable to complete the prolonged sarcomere length control protocols necessary to measure the recovery time-courses at different levels of $Ca^{2+}$ activation.

This work presents results from a new series of experiments. We used permeabilized rat soleus (slow twitch) muscle fibers (instead of fast twitch rabbit psoas preparations) and were consequently able to maintain sarcomere length control for extended periods of time. Some of the fibers used in these experiments withstood more than 250 trials (500 triangular length changes imposed under sarcomere length control) in $Ca^{2+}$ concentrations ranging from pCa 6.5 (minimal activation) to pCa 4.5 (saturating effect) without substantial deterioration of their appearance or mechanical response. The robust nature of these preparations allowed us to establish the $Ca^{2+}$ dependence of the stiffness recovery rate.

A brief account of the experimental results has been presented to the Biophysical Society (Campbell and Moss, 2001).

## METHODS

### Fiber preparations

Female Sprague-Dawley rats (200–224 g) were anesthetized by inhalation of 3 to 4% methoxyflurane and subsequently killed by a pneumothorax. The soleus muscles were isolated, and bundles of $\sim$20 fibers were tied to glass capillary tubes and skinned for 4 to 6 h at 4°C in relaxing solution (100 mM KCl, 20 mM imidazole, 4 mM MgATP, 2 mM EGTA, and 1 mM free $Mg^{2+}$) containing 1% (v/v) Triton X-100. Bundles were stored at −20°C in relaxing solution containing 50% (v/v) glycerol for up to 3 weeks. Animal use was approved by the University of Wisconsin-Madison Animal Care Committee.

### Experimental apparatus

The experimental apparatus was similar to that described by Campbell and Moss (2000). A schematic diagram is shown in Fig. 1 *A*. A segment of a single muscle fiber (mean length 970 $\mu$m, width 83 $\mu$m) was attached between a force transducer (Model 403, Aurora Scientific Inc., Ontario, Canada, resonant frequency $\sim$600 Hz) and a motor (Model 6350, Cambridge Technology Inc., Cambridge, MA, time for 100-$\mu$m step $\sim$1 ms) and activated in solutions with free $Ca^{2+}$ concentrations ranging from pCa ($= -\log_{10}[Ca^{2+}]$) 6.5 to 4.5. The mean sarcomere length in the center of the muscle was measured by laser diffraction. Force, sarcomere length, and motor position (proportional to the length of the fiber segment) were sampled (12-bit resolution) at 1 kHz and saved to computer files for later analysis. The ends of some (but not all) preparations were "fixed" with gluteraldehyde (Fig. 1 *B*) in an attempt to further minimize series compliance (Campbell and Moss, 2000). No substantial differences were apparent in the present experiments between the properties of "fixed" and "unfixed" fibers.

### Solutions

pCa solutions (pH 7.0 at 15°C) contained 20 mM imidazole, 14.5 mM creatine phosphate, 7 mM EGTA, 4 mM MgATP, 1 mM free $Mg^{2+}$, free $Ca^{2+}$ ranging from 1 nM (pCa 9.0) to 32 $\mu$M (pCa 4.5) and sufficient KCl to adjust the ionic strength to 180 mM. Preactivating solution was identical to pCa 9.0 solution except that EGTA was reduced to 0.5 mM and 6.5 mM HDTA was added. The final concentrations of each metal, ligand, and metal-ligand complex were calculated using the computer program developed by Fabiato (1988), and the stability constants listed by Godt and Lindley (1982).

### Protocol

At the beginning of each experiment, the fiber segment was immersed in pCa 9.0 solution (negligible $Ca^{2+}$ concentration), and the position of the motor was adjusted until the mean sarcomere length in the center of the fiber segment was $\sim$2.6 $\mu$m (Fig. 1*C*). The cross-sectional area of the fiber (assuming a circular profile) was then determined by video microscopy. When these measurements were complete the muscle was immersed for 45 s in preactivating solution (with a reduced $Ca^{2+}$ buffering capacity) and

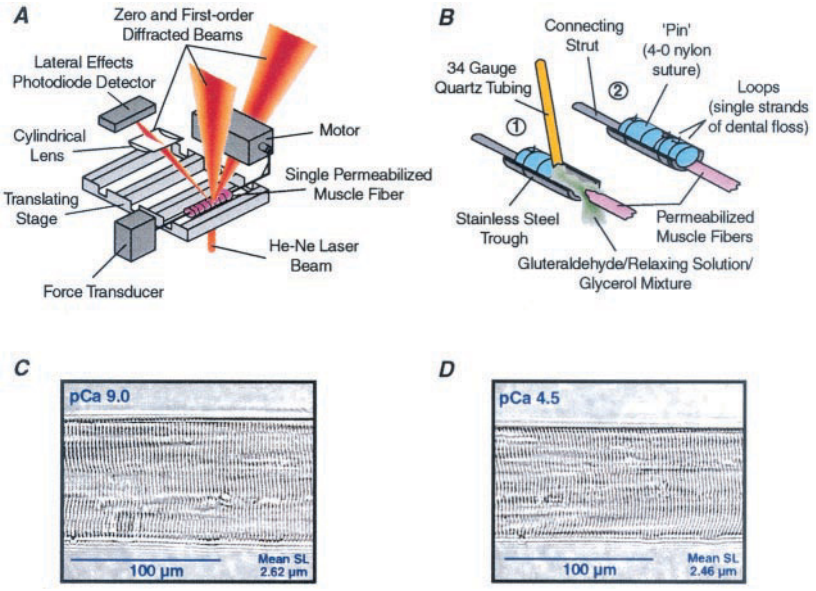


FIGURE 1 Methods. (*A*) Experimental apparatus. Chemically permeabilized rat soleus muscle fibers were connected between a force transducer and a motor. A HeNe laser beam was projected through the center of the preparation, and one of the first order diffraction beams was imaged onto a position sensitive detector for feedback control. (*B*) Gluteraldehyde fixation. Each end of the fiber was 1) "fixed" with a solution containing gluteraldehyde/relaxing solution/glycerol, (1:10:10, v/v) and 2) secured with a second "pin" positioned as close as possible to the end of the trough and tied in place with two strands of dental floss. (*C* and *D*) Photomicrographs. Stable striation patterns were maintained at all levels of $Ca^{2+}$ activation. Shortening at maximal $Ca^{2+}$ activation ranged from 4 to 9% in five preparations.

then immediately transferred to maximally activating pCa 4.5 solution. Once tension had reached a steady state, the video image was checked to ensure that the muscle striation pattern remained stationary and that sarcomere shortening had not exceeded 10%. In the present experiments, sarcomere length in the central region of the fiber in pCa 4.5 solution shortened by between 4 and 9% of the pCa 9.0 value (Fig. 1 *D*). The muscle was then returned to pCa 9.0 solution.

If any abnormalities were apparent, the fiber was discarded at this point. Otherwise the fiber was returned (via preactivating solution) to an activating solution with a pCa value randomly selected within the range 6.5 to 4.5. Data recordings were initiated at regular 20-s intervals and were normally obtained in sets of 11 trials.

Each individual trial lasted 10 s and followed a set pattern (Fig. 2) commencing with a 100-ms interval during which the motor position (and thus the fiber length) was held constant. After this initial recording period, the experiment switched to sarcomere length control. In this mode the motor command voltage was updated at 1-ms intervals by a computer (an Intel 486 processor using Assembly language routines to implement real-time control) using a feedback signal derived from the position of the diffracted laser beam on the photo-diode detector (Fig. 1 *A*). This procedure controlled the mean sarcomere length in the center of the preparation and minimized any potential artifacts due to compliance near the ends of the preparation. This phase of the trial commenced with a 100-ms recording period during which the striation pattern was held stationary at the prevailing sarcomere length. A triangular length change (paired ramp stretch and release, 0.03 $l_0$, $\pm$ 0.1 $l_0$ $s^{-1}$ in which $l_0$ is the initial fiber length) was then imposed under sarcomere length control, after which the striation pattern was again held stationary for an interval, which ranged from 1 ms to 7 s in different trials. A second identical triangular length change was then imposed. The recording continued with a further 100-ms period at fixed sarcomere length after which the experiment switched back to motor (fiber length) control. The muscle was immediately shortened by 0.2 $l_0$, held at this short length for 20 ms, and then rapidly reextended to the original fiber length. Data recording continued for the remainder of the 10-s trial.

Multiple recordings were obtained from each fiber in each $Ca^{2+}$ activating solution. Individual trials differed only in their intertriangle interval, which was adjusted from 1 to 7000 ms in the following order: 7000, 1000, 100, 10, 1, 200, 20, 3000, 500, 50, 5 ms. In most cases, 3 sets of 11 trials

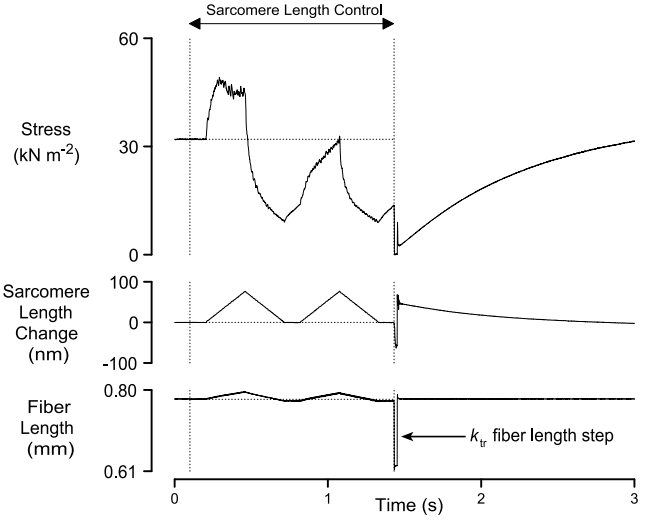


FIGURE 2 Single experimental trial. pCa 6.0. (Steady-state tension 0.46 of maximum in pCa 4.5 solution). Length change 0.03 $l_0$, velocity $\pm$ 0.12 $l_0$ $s^{-1}$, intertriangle interval 0.1 s. The sarcomere length signal is invalid during the $k_{tr}$ step (0.2 $l_0$, 20-ms duration) because the imposed length change is sufficiently large to move the diffracted laser beam off the position sensitive detector. In all subsequent data records, sarcomere and fiber length records are clipped to the graph axes during the $k_{tr}$ step so that the quality of the sarcomere length control can be more readily assessed.

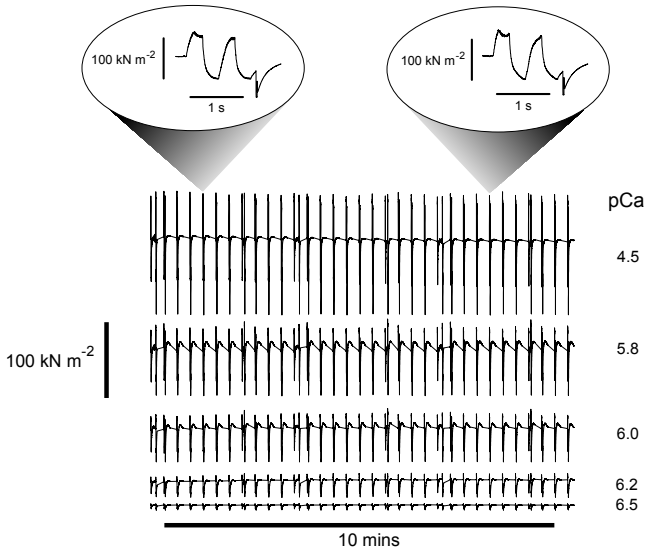


FIGURE 3 Slow time-base recording of experimental protocol. Traces show slow time-base tension records (reconstructed from computer files recorded during consecutive trials) for 3 sets of 11 trials carried out at each of five different levels of $Ca^{2+}$ activation. Insets show trials with identical intertriangle intervals (1 ms) recorded near the beginning and end of a maximal $Ca^{2+}$ activation. Only minimal differences between the recordings are apparent even though the second trial was initiated 7 min after the first.

were recorded before the fiber was returned to pCa 9.0 solution. Some fibers could withstand more than 250 trials at different levels of $Ca^{2+}$ activation without deterioration of their appearance or mechanical properties (Fig. 3).

In most cases, trials with equal intertriangle intervals were averaged at each level of $Ca^{2+}$ activation to improve the signal-to-noise ratio and minimize any slight trends in the consecutive data records. Summary results presented in this paper represent data obtained from ~1000 trials using five different fiber preparations from one rat. Qualitatively similar results have been obtained from 10 other fiber preparations from a number of different rats. Data analysis was performed using programs custom written in C. Results are reported as mean ± SE unless otherwise stated.

## Theoretical modeling

We used computer simulations of cross-bridges cycling through the scheme illustrated in Fig. 11 to investigate whether this type of theoretical model may be consistent with the present experimental results. The mathematics and numerical procedures underlying the calculations are identical to those described previously (Campbell and Moss, 2000) with the exception that in the present simulations we chose to use detachment rate constants $k_{-1}(x)$ and $k_3(x)$, which had a simpler functional dependence on the cross-bridge displacement.

The theoretical model was defined by 14 parameters (Table 1). We used multidimensional minimization routines, which continually adjusted the parameter values in an attempt to find the minimal possible $\chi^2$ error between the simulated force response and selected experimental records. In our previous paper (Campbell and Moss, 2000) we used either Powell's method or simplex algorithms (Press et al., 1992) to optimize the simula-

**TABLE 1 Optimized simulation parameters**

| | | Units |
|---|---|---|
| Rate constants | | |
| $k_1(x)$ | $1.57 \times 10^{10} \times \exp\left(-\frac{\kappa_{cb} \times x^2}{2 \times k_B \times T}\right)$ | $s^{-1}\ m^{-1}$ |
| $k_{-1}(x)$ | $57.7 + 2.68 \times 10^{18} \times x^2 \quad x \geq 0$<br>$57.7 + 4.18 \times 10^{19} \times x^2 \quad x < 0$ | $s^{-1}$<br>$s^{-1}$ |
| $k_2(x)$ | $0.698 + 1.503 \times \frac{\exp\left(-\frac{\kappa_{cb} \times x_{ps} \times (-x + x_{ps}/2)}{k_B \times T}\right)}{1 + \exp\left(-\frac{\kappa_{cb} \times x_{ps} \times (-x + x_{ps}/2)}{k_B \times T}\right)}$ | $s^{-1}$ |
| $k_{-2}(x)$ | $\frac{1.41}{1 + \exp\left(-\frac{\kappa_{cb} \times x_{ps} \times (-x - x_{ps}/2}{k_B \times T}\right)}$ | $s^{-1}$ |
| $k_3(x)$ | $3.45 + 2.00 \times 10^{16} \times x^2 \quad x \geq 0$<br>$3.45 + 6.63 \times 10^{19} \times x^2 \quad x < 0$ | $s^{-1}$<br>$s^{-1}$ |
| Cross-bridge Parameters | | |
| $\kappa_{cb}$ | $1.88 \times 10^{-4}$ N m$^{-1}$ | |
| $x_{ps}$ | $4.83 \times 10^{-9}$ m | |
| Parallel Component Parameters | | |
| $\sigma_P$ | 9980 N m$^{-2}$ | |
| L | $2.72 \times 10^{-8}$ m | |
| Constants | | |
| Cross-bridge number density* | $2.19 \times 10^{17}$ | |
| Temperature, $T$ | 288 K | |
| Boltzmann's constant, $k_B$ | $1.38 \times 10^{-23}$ J K$^{-1}$ | |

*Number of cross-bridges in a theoretical "half-sarcomere" of unit cross-sectional area and length 1.3 $\mu$m if the concentration of cross-bridges is 0.28 mM (Slawnych et al., 1994). Other parameters are as defined in the appendix of Campbell and Moss, 2000. Rate equations assume cross-bridge displacements $x$ are expressed in meters.

tions. On this occasion we used a slightly more sophisticated approach, performing repeated Powell or simplex minimizations, interposed by random jumps to new regions of parameter space. The size of the random jump was reduced after each iteration, a procedure described as "simulated annealing" (Press et al., 1992). This approach ensures that regions of parameter space corresponding to low $\chi^2$ errors are investigated in increasing detail without the routine becoming "trapped" in local minima during the initial iterations.

Simulations were performed on Pentium PCs using source code developed in Visual C++. Optimizations generally converged to minimal $\chi^2$ values after $\sim 10^5$ iterations.

## RESULTS

Rat soleus fibers were activated in solutions with free $Ca^{2+}$ concentrations ranging from pCa 6.5 (minimal activation) to pCa 4.5 (saturating effect) and subjected to repeated triangular length changes (paired ramp stretches and releases, length change 0.03 $l_0$, velocity $\pm$ 0.10–0.12 $l_0$ $s^{-1}$ in different preparations). Fig. 2 shows a typical experimental record.

When the fiber was first stretched, tension rose sharply reaching a peak value after a movement of ~15 nm half-sarcomere$^{-1}$. Tension then fell slightly to a plateau that was maintained during the remainder of the stretch. This biphasic response is well known and has been studied by a number of other workers using a variety of different muscle preparations (Lombardi and Piazzesi, 1990; Stienen et al., 1992; Getz et al., 1998, Edman, 1999).

In our experiments, the fiber was returned to its original sarcomere length during the second half of the triangular length change. During this phase of the movement, tension fell to a minimum, which was generally only ~0.25 of the steady-state value. As soon as shortening ceased, tension started to recover toward the steady-state value, but in the example shown in Fig. 2 this process was interrupted by a second triangular length change. Although tension again rose sharply during the initial phase of the movement, the magnitude of the response was substantially less than during the first stretch. When the fiber was again returned to its original sarcomere length, tension fell once more with a similar profile to that produced during the first length change. If a third length change was imposed, the response was almost identical to that produced during the second movement (data not shown) (Campbell and Moss, 2000).

Although these general features were observed at each level of $Ca^{2+}$ activation, the precise form of the second stretch response depended on the time interval between the triangular length changes. We measured the recovery time course by imposing multiple paired length changes separated by different time intervals at each level of $Ca^{2+}$ activation. Individual trials were initiated at regular 20-s intervals, a period which ensured that each experiment was preceded by a recovery time of at least 12 s without imposed movements. Because experimental results presented later in this paper show that tension responses separated by 7 s are virtually indistinguishable, we are confident that individual recordings are unaffected by preceding measurements. Mechanical responses recorded near the beginning and end of each $Ca^{2+}$ activation were compared during the analysis procedures, and recordings were discarded if substantial changes were apparent during the activation or if sarcomere length control had become compromised.

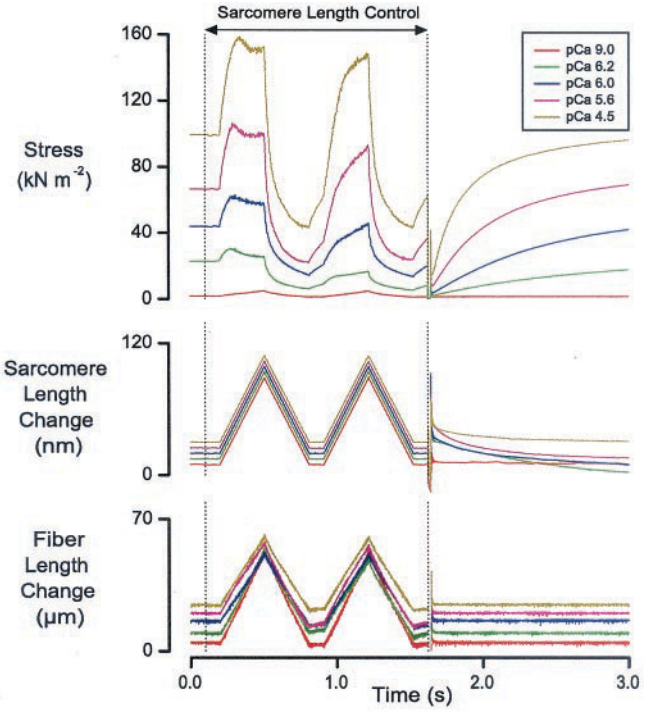


FIGURE 4 $Ca^{2+}$-dependence. Length change 0.03 $l_0$, velocity $\pm$ 0.10 $l_0$ $s^{-1}$, intertriangle separation 0.1 s. Sarcomere and fiber length records are offset for clarity.

### First stretch $Ca^{2+}$ dependence

Fig. 4 is a superposition of experimental records obtained from one fiber at five different levels of $Ca^{2+}$ activation. This form of presentation emphasizes two important points about our experimental results: 1) the magnitude of the tension response to movement increased with the free $Ca^{2+}$ concentration in the activating solution and 2) the qualitative shape of the first stretch tension response was preserved at each activating $Ca^{2+}$ concentration i.e., when the fiber was immersed in a solution with a pCa $\leq$ 6.5, the stretch always resulted in an initial rapid rise in tension followed by a slight drop to a plateau that was maintained during the remainder of the stretch.

This characteristic transient/plateau response is systematically different from the response measured when the fiber was stretched in pCa 9.0 solution (negligible free $Ca^{2+}$ concentration). Under these relaxing conditions, tension increased roughly linearly throughout the imposed stretch,

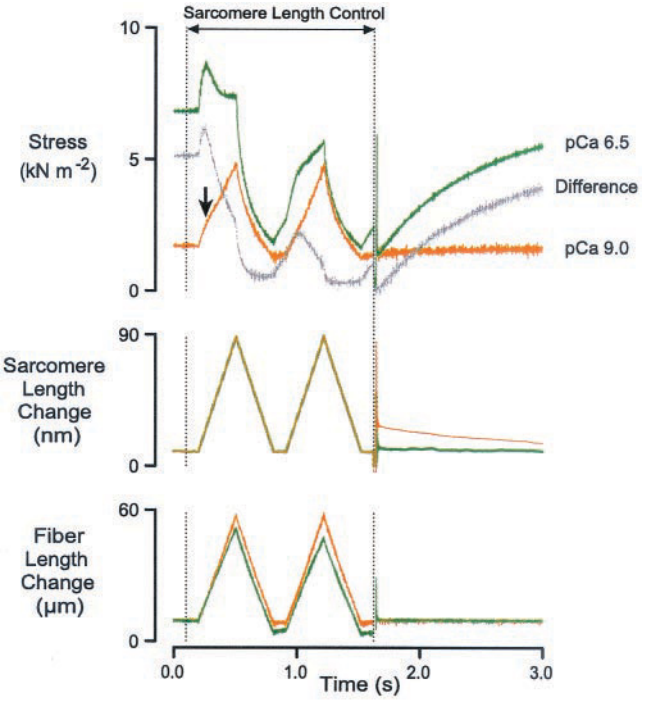


FIGURE 5 Low level $Ca^{2+}$-activation. pCa 9.0 and pCa 6.5 records from the same fiber shown in Fig. 4. The arrow marks a slight discontinuity in the pCa 9.0 tension record. The difference between the pCa 6.5 and pCa 9.0 tension records is shown in gray.

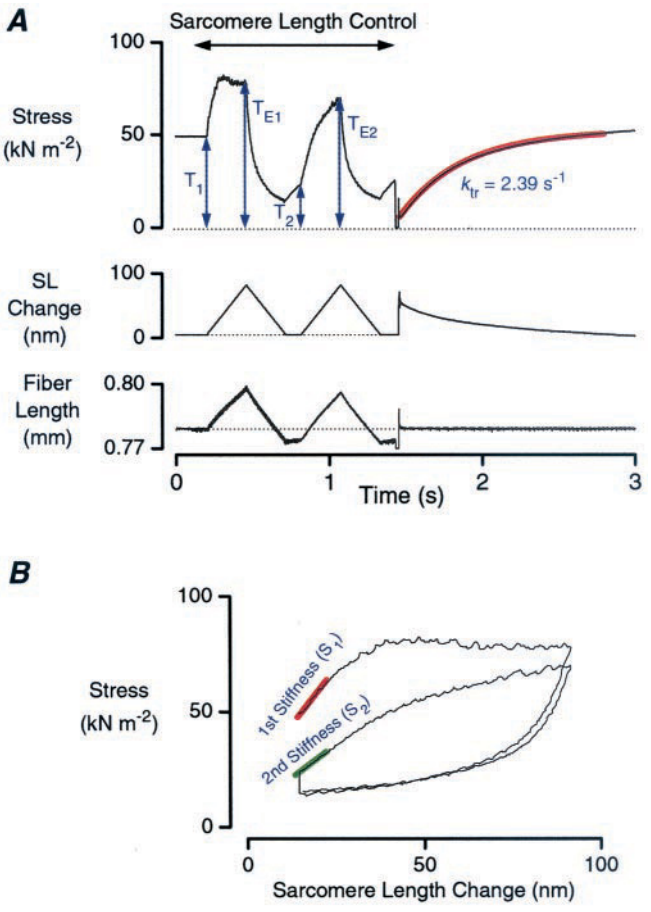


FIGURE 6 Analysis. pCa 5.6 (steady-state tension 0.72 of maximum in pCa 4.5). Length change 0.03 $l_0$, velocity ± 0.12 $l_0$ $s^{-1}$, intertriangle separation 0.1 s. (*A*) Tension. Individual trials consisted of two triangular length changes followed by a rapid shortening/restretch maneuver (0.2 $l_0$, 20-ms step duration). Tension recovery during the intertriangle interval (Figs. 8 and 9) was assessed by defining "relative tension" ($T_R$) as the ratio of the tension at the commencement of the second stretch to the steady-state isometric value, i.e., $T_2/T_1$. In this example $T_R$ was equal to 0.47. The tensions at the end of the first and second stretches were designated $T_{E1}$ and $T_{E2}$, respectively. "Relative tension plateau" (Fig. 7 *D*) was defined as $T_{E1}/T_1$ and in this record was equal to 1.57. The rate of tension regeneration ($k_{tr}$) after each step length change was calculated by fitting a line of the form $y = a \times [1 - \exp(-k_{tr} \times t)]$ to the measured response. In this example the fit is illustrated by the overlaid red line. (*B*) Stiffness. Muscle stiffness during the initial phase of each triangular length change was calculated from the gradient of a regression line fitted to the first 25 ms of an *xy* plot of tension against sarcomere length. Relative stiffness ($S_R$) was calculated as the second stretch stiffness divided by the corresponding first stretch value. In this example the first and second stretch stiffness values are indicated by the gradients of the red and green lines, respectively. $S_R$ was equal to 0.59. The break length ($\Delta L$, Fig. 7 *C*) was defined as the ratio of the maximal initial phase tension to the first stretch stiffness (as illustrated in Fig. 5 of Campbell and Moss, 2000) and was expressed in units of nanometers extension per half-sarcomere.

and the response was similar to that which might be expected from a simple elastic system (Fig. 5). Although this work is primarily concerned with the mechanical properties of $Ca^{2+}$ activated fibers, the pCa 9.0 response is important in this study because it probably reflects the properties of the endosarcomeric (e.g., titin, nebulin, and desmin proteins) and exosarcomeric lattice structures (e.g., collagen fibrils and intermediate filaments) (Price, 1991).

We believe that the tension response of a $Ca^{2+}$ activated fiber is the sum of two components that add in parallel (see Fig. 9 *A* of Campbell and Moss, 2000). The first of these components is the force produced by displacing populations of cycling cross-bridges; the second is the tension response of the lattice structures. If this hypothesis is correct and the passive lattice component is independent of the intracellular free $Ca^{2+}$ concentration (see Discussion), the cross-bridge component can be calculated as the difference between the measured response in the $Ca^{2+}$-activated fiber and the passive response measured in pCa 9.0 solution (Fig. 5).

Although the mechanical response of the fiber in pCa 9.0 solution is interesting (and discussed in considerable detail later in this paper), it forms quite a small part of the initial phase of the response in a $Ca^{2+}$-activated fiber. Consider for example the experimental records shown in Fig. 5; the stiffness of the muscle (calculated as in Fig. 6 *B*) was more than three times as great when it was activated in pCa 6.5 solution ($P/P_0 = 0.07$) than when it was stretched in pCa 9.0 solution. At higher levels of $Ca^{2+}$ activation, the pCa 9.0 stiffness forms an even smaller portion of the measured response. Fig. 7 *B* shows the initial stiffness of muscle fibers activated in solutions with pCa ≤ 6.5 plotted against steady-

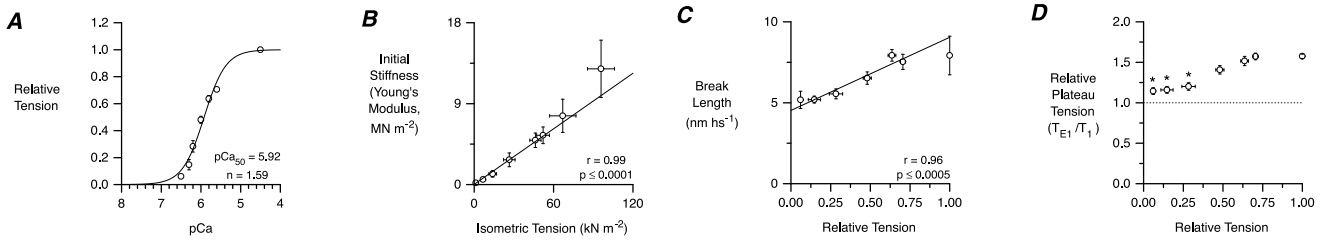


FIGURE 7 First stretch $Ca^{2+}$-dependence. (*A*) pCa-tension. Symbols show mean (±SE) $Ca^{2+}$-activated tension expressed relative to maximal pCa 4.5 value. Line is a best fit of the form $y = [Ca^{2+}]^n/([Ca^{2+}]^n + [Ca_{50}{}^{2+}]^n)$. (*B*) Stiffness. The first stretch initial stiffness increased in proportion with the steady-state isometric tension as the pCa of the activating solution was reduced from pCa 6.5 to 4.5. (*C*) Break length. The length of the initial phase of the tension response increased with the level of $Ca^{2+}$ activation. (*D*) Relative tension plateau. The relative plateau tension ($T_{E1}/T_1$) was increased at high levels of $Ca^{2+}$ activation. Points marked by ⋆ are statistically different from the pCa 4.5 value ($p < 0.05$, one-way ANOVA, Student-Neuman-Keuls post-hoc comparison).

state isometric tension ($Ca^{2+}$ dependence shown in Fig. 7 *A*). A regression line fitted to the experimental values extrapolates to a point very near the origin. If the initial stiffness measured in pCa 9.0 solution formed a substantial proportion of the measured response in $Ca^{2+}$ activated fibers, the regression line would have had a significant positive $y$ intercept.

The break length ($\Delta L$) of the mechanical response (defined in the legend of Fig. 6) is indicative of the extent of interfilamentary movement at the transition between the first and second phases of the tension response. $\Delta L$ ranged from 4.4 to 9.9 nm half-sarcomere$^{-1}$ in different preparations and showed an upward trend with increasing $Ca^{2+}$ concentration, which was statistically significant although the data from individual preparations was somewhat variable.

The data presented in Fig. 7, *B* and *C* qualitatively confirm two important findings from our previous experiments using rabbit psoas fibers (Campbell and Moss, 2000). Fig. 7 *D* presents the results of new measurements, which we were unable to make in the original experiments. In rabbit psoas fibers, tension dropped slightly at the end of the initial phase of the tension response and then continued to rise slowly during the remainder of the stretch. In contrast, in the present experiments tension was maintained at an approximately constant plateau during the latter stages of the first stretch. Fig. 7 *D* shows that the relative height of this plateau ($T_{E1}/T_1$, defined in Fig. 6 *A*) increased with the level of $Ca^{2+}$ activation. The mean values of the pCa 4.5 data points were significantly higher than the pCa 6.5, pCa 6.3, and pCa 6.2 values ($p < 0.05$, one-way ANOVA, Student-Neuman-Keuls post-hoc comparison).

## History dependence

Tension and sarcomere length records for different intertriangle intervals are shown in Fig. 8. At each level of $Ca^{2+}$ activation the initial phase of the second stretch response was diminished for short intertriangle intervals. As the interval was prolonged, the second stretch response increased in size and when the interval reached 7 s, the first and second stretch responses were virtually indistinguishable. The time course of this progressive recovery was analyzed for each level of $Ca^{2+}$ activation using the procedures illustrated in Fig. 6. The initial stiffness of the muscle was calculated for each stretch and relative stiffness ($S_R$) was defined as $S_2/S_1$ for each intertriangle interval. Relative tension ($T_R$) was defined in a similar manner as $T_2/T_1$. Plots of the mean values of $S_R$ and $T_R$ from different preparations are shown for the full range of intertriangle intervals in Fig. 8.

$S_R$ and $T_R$ recovered progressively with increasing intertriangle intervals (Fig. 8) in activated fibers (pCa ≤ 6.5). Curves of the form $y = [\, a - b \times \exp(-c \times \Delta t)\, ]$ in which $a$ and $b$ are constants, $c$ is the rate of recovery, and $\Delta t$ is the intertriangle interval fitted both parameters reasonably well although two systematic differences between the recovery time-courses were apparent. $T_R$ was always reduced by a greater amount than $S_R$ for short intervals and was always slightly better fit by the exponential curve. The difference in the accuracy of the fits reflects that fact that $T_R$ values continued to drop as the intertriangle interval was reduced toward 1 ms, whereas the $S_R$ values tended to plateau or even rise slightly for intervals below ~100 ms.

To our initial surprise, the recovery time courses remained remarkably consistent as the level of $Ca^{2+}$ activation was increased (Fig. 8). There was some variation in the maximal stiffness reduction at different levels of $Ca^{2+}$ activation and the recovery time courses became faster at higher levels of activation but the effects were modest compared with the increase in steady-state isometric tension. The rate of relative stiffness recovery ($S_R$) increased from 0.89 ± 0.13 s$^{-1}$ at pCa 6.5 to 1.77 ± 0.25 s$^{-1}$ at pCa 4.5. The corresponding change for the rate of relative tension recovery ($T_R$) was 1.51 ± 0.15 s$^{-1}$ to 3.50 ± 0.09 s$^{-1}$. Steady-state isometric tension increased 17-fold over the same range of $Ca^{2+}$ concentrations.

The recovery rates of $T_R$ and $S_R$ are plotted against the corresponding relative isometric tension in Fig. 9. Also shown in the figure are the values of $k_{tr}$, the rates of tension recovery (Fig. 6 *A*) after the slack-step imposed after each

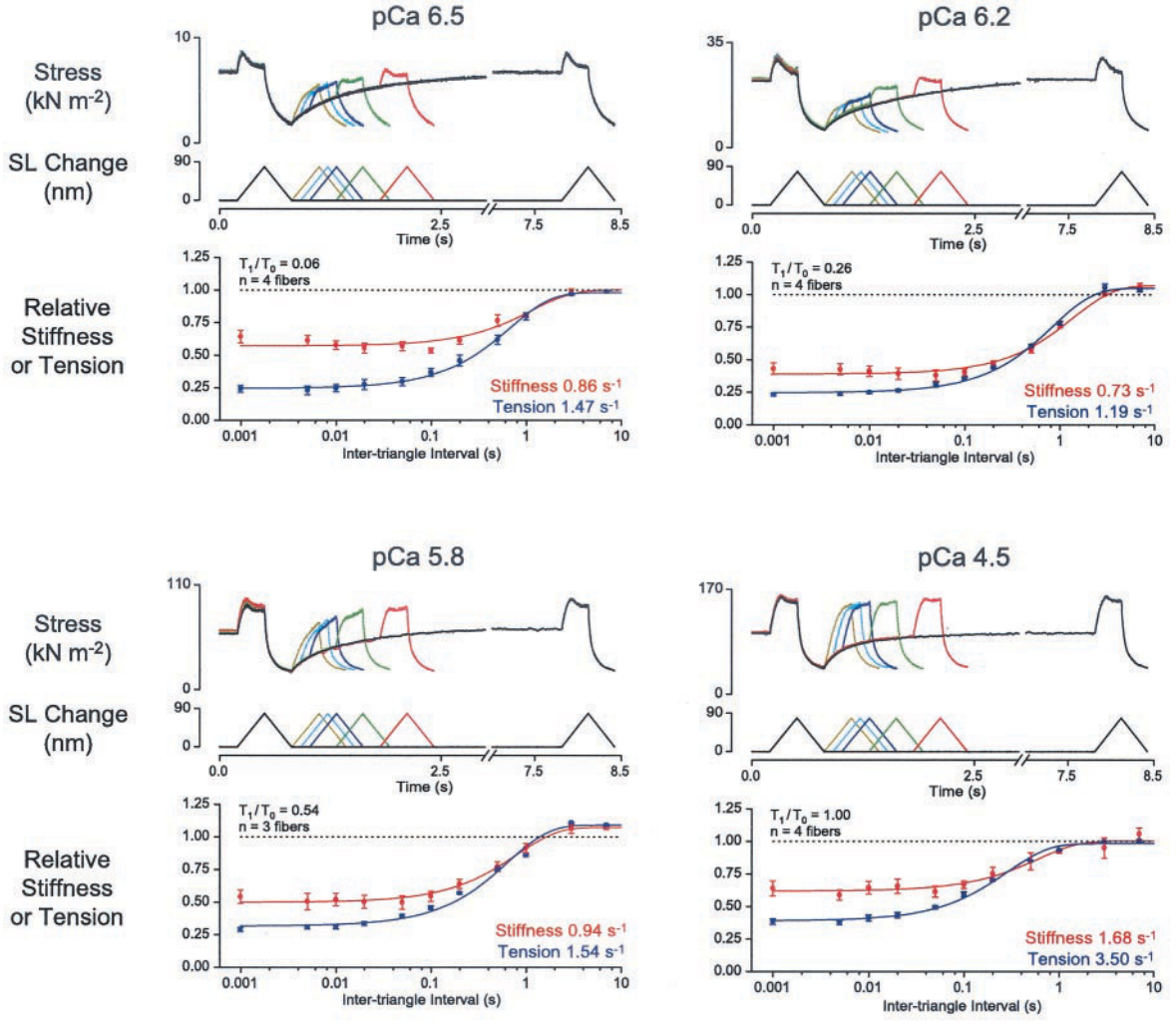


FIGURE 8 Recovery time-courses of relative stiffness and relative tension. Superimposed tension and sarcomere length records. Experimental records from a single representative fiber. Length change 0.03 $l_0$, velocity ± 0.10 $l_0$ $s^{-1}$. Records show superimposed tension and sarcomere length records at a range of different activating $Ca^{2+}$ concentrations for trials with intertriangle intervals ranging from 1 ms to 7 s. Responses separated by 7 s are virtually indistinguishable. The mean level of $Ca^{2+}$ activation in each pCa solution is given by the ratio $T_1/T_0$ i.e., the steady-state isometric tension expressed relative to the corresponding value in saturating pCa 4.5 solution. Note that 1) each stress $y$ axis has a different scale, and 2) there is a break between 2.5 and 7.5 s in the time axis in each panel. Recovery time course. Symbols show the mean (±SE) relative stiffness ($S_R$, *red*) and relative tension ($T_R$, *blue*) observed for each intertriangle interval at each activating $Ca^{2+}$ concentration. Continuous lines are the best fit of the form $y = [\, a - b \times \exp(-c \times \Delta t)]$ for each parameter where $a$ and $b$ are constants, $c$ is the rate of recovery, and $\Delta t$ is the intertriangle interval. Note that the $x$ axis has a logarithmic scale.

paired length change. (For comparison, the maximal value of $k_{tr}$ (3.8 ± 0.1 $s^{-1}$) in the present experiments is similar to that found in an earlier study (3.0 ± 0.1 $s^{-1}$, Metzger and Moss (1990) from our laboratory.) All three parameters dip at a relative tension of 0.28 (pCa 6.2) and increase at higher levels of $Ca^{2+}$ activation. Two features of this plot are worthy of particular note. First, the values of $k_{tr}$ and the rates of $T_R$ recovery scale in a similar way as the free $Ca^{2+}$ concentration is increased from minimum to saturating values. This is consistent with the hypothesis that both parameters measure the rate at which cross-bridges accumulate in force-generating states after a perturbation (Brenner, 1988) even though the measurement protocols are quite different. Second, the rates of $T_R$ and $S_R$ recovery are very different at the highest level of $Ca^{2+}$ activation. The probability that the observed difference occurs by chance is less than 0.001 (Student's $t$-test, independent samples).

## Plateau tension

Although the recovery time courses of the $S_R$ and $T_R$ parameters are only affected to a minor degree (≤ threefold increase in rate) by increasing $Ca^{2+}$ concentrations, the form of the second stretch tension response is critically dependent on the level of $Ca^{2+}$ activation. The effect can be

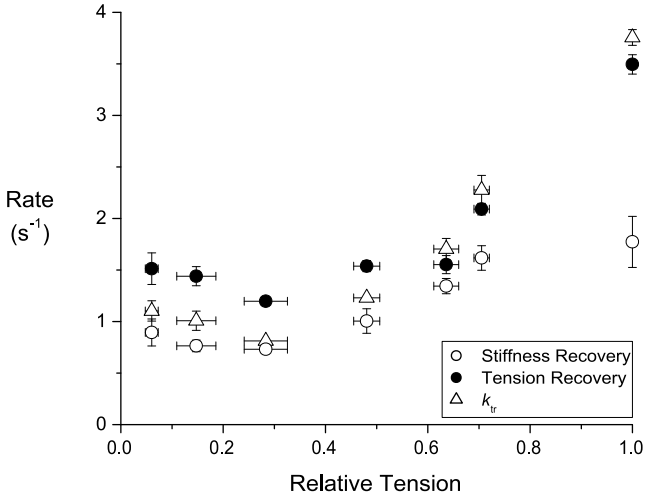


FIGURE 9 Recovery rates. Symbols show the mean (±SE) values ($n$ = 3–5 preparations at different pCa values) for the rates of recovery of relative stiffness ($S_R$, ○), relative tension ($T_R$, ●), and $k_{tr}$ (△) plotted against relative isometric tension.

seen in the experimental records in Fig. 8. At low levels of $Ca^{2+}$ activation, the maximal tension produced during the second movement is substantially less than the first stretch tension plateau for short intertriangle intervals. In many cases, the maximal second stretch tension does not even reach the steady isometric level. (An example of this type of response is shown in greater detail in Fig. 5.) This contrasts with the behavior at high levels of $Ca^{2+}$ activation where the tensions at the end of the first and second stretches are almost identical.

Fig. 10 presents a quantitative analysis of the effect.

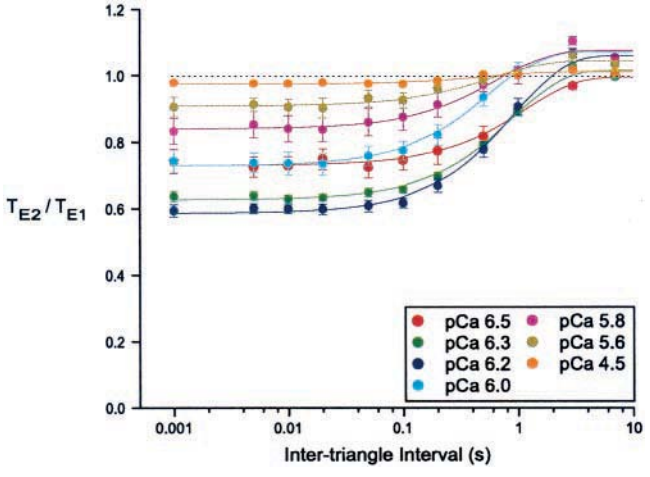


FIGURE 10 Second stretch plateau recovery. Symbols show the mean (±SE) values ($n$ = 3–5 preparations at different $Ca^{2+}$ concentrations) of the relative tension at the end of the second stretch ($T_{E2}/T_{E1}$) plotted against the corresponding intertriangle interval. Continuous lines are best fits of the form $y = [a - b \times \exp(-c \times \Delta t)]$ in which $a$ and $b$ are constants, $c$ is the rate of recovery, and $\Delta t$ is the intertriangle interval.

Different colored symbols show the relative tension at the end of the second stretch ($T_{E2}/T_{E1}$) plotted against the corresponding intertriangle interval for each level of $Ca^{2+}$ activation. At low $Ca^{2+}$ concentrations, $T_{E2}/T_{E1}$ is reduced for short intertriangle intervals and recovers toward unity with an exponential time course. At high levels of $Ca^{2+}$ activation, $T_{E2}/T_{E1}$ remains roughly constant and is almost unaffected by the time interval between the triangular length changes.

## Theoretical simulations

The initial stiffness of the first stretch response increased ~23-fold (from a Young's Modulus of 0.56 ± 0.16 MN $m^{-2}$ to 12.87 ± 3.19 MN $m^{-2}$) when the level of $Ca^{2+}$ activation was raised from pCa 6.5 to 4.5. Despite this large increase in the magnitude of the response, the relative reduction in stiffness after movement remained roughly constant. $S_R$ was always reduced by approximately one-half, independent of the level of $Ca^{2+}$ activation, when the second stretch followed immediately after the first (Fig. 8). This finding suggests that the history dependence of the mechanical properties is inherent to the contractile apparatus and is therefore consistent with our original suggestion (Campbell and Moss, 2000) that the reduced stiffness and tension after movement reflect a temporary decrease in the number of cross-bridges attached between the thick and thin filaments.

If this hypothesis is correct, it should be possible to simulate the muscle's history-dependent properties with a simple cross-bridge model. In our previous paper (Campbell and Moss, 2000), we showed that cross-bridges cycling through the scheme illustrated in Fig. 11 could account for the thixotropic properties of a submaximally activated rabbit psoas fiber. The results of simulations presented in Figs. 12 and 13 show that the cross-bridge hypothesis is also consistent with the history-dependent properties of maximally activated rat soleus fibers. The model was defined by 14 parameters, and Fig. 12 shows the simulated response when these parameters were judiciously adjusted to match the pCa 4.5 experimental response shown in Fig. 4. The corresponding simulation variables are shown in Table 1.

Fig. 13 shows the results of simulations based on these parameters for paired triangular length changes with intertriangle intervals ranging from 1 ms to 7 s. Although the simulated recovery time-courses are not identical to those measured experimentally they do exhibit two important qualitative features of the experimental traces (Fig. 8, bottom right panel). 1) $T_R$ is reduced by a greater amount than $S_R$ for short intertriangle intervals, and 2) $T_R$ is well fit by an exponential curve, whereas $S_R$ values rise slightly when the intertriangle interval is reduced to very short periods. We believe that the complementary features present in the experimental records and the simulated recovery time-

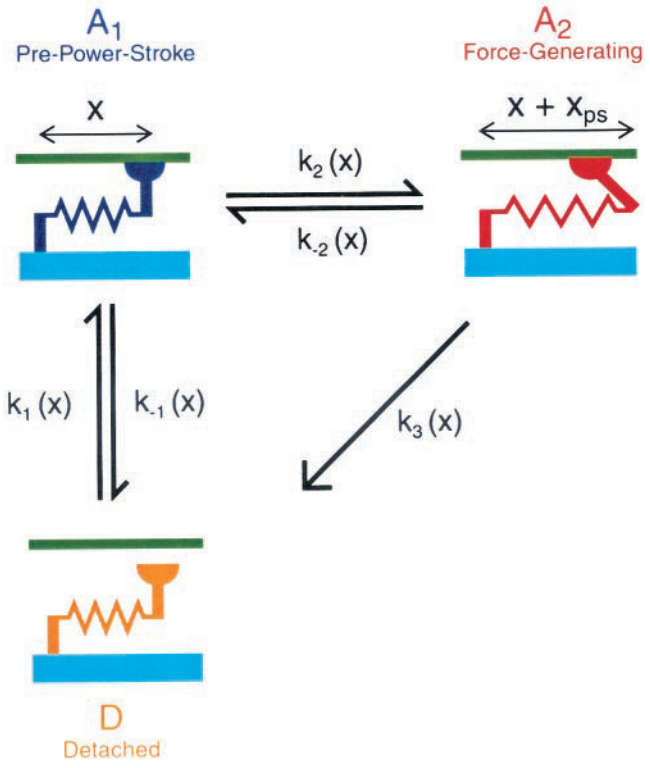


FIGURE 11 Cross-bridge model. Cross-bridges are assumed to act as linear elastic elements (stiffness $\kappa_{cb}$) and cycle independently through three distinct states: D, detached; $A_1$, first attached; $A_2$, second attached. The rate constants defining the probability of a cross-bridge undergoing a transition between the different states depend on the length $x$ of the cross-bridge's elastic element (referred to as the cross-bridge displacement). The transition between the $A_1$ and $A_2$ states represents a force-generating power stroke. Cross-bridges attached in the $A_1$ and $A_2$ states produce forces equal to $\kappa_{cb} \times x$ and $\kappa_{cb} \times (x + x_{ps})$, respectively.

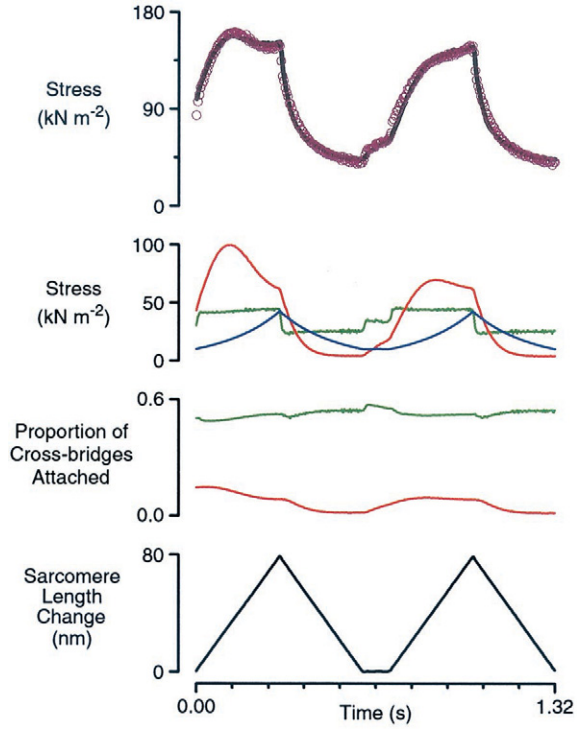


FIGURE 12 Simulated mechanical response to two triangular length changes. Stress records. Experimental record (pCa 4.5, length change 0.03 $l_0$, $\pm$ 0.10 $l_0$ $s^{-1}$, the same record is shown in Fig. 4) (*solid black line*). Simulated response (*open circles*). Force due to cross-bridges in $A_1$ state (*green line*). Force due to cross-bridges in $A_2$ state (*red line*). Force due to passive component (*blue line*). Proportion of cross-bridges attached. $A_1$ state (*green line*). $A_2$ state (*red line*). The simulated fit represents the lowest $\chi^2$ error ($\Sigma(y_{sim} - y_{expt})^2$), which we were able to find for the full 1.32-s record and represents the best "mathematical" fit between the simulated and experimental traces when every data point is considered to be of equal importance. The maximal deviation between the experimental and simulated values (16%) occurs at the first point and corresponds to an underestimate of the steady-state isometric tension. In alternative calculations the simulations could have been constrained to this value by assigning a higher weight to the error calculation for the first data point. This would have improved the estimate of isometric tension but worsened the overall fit.

courses provide strong support for the cross-bridge hypothesis.

## DISCUSSION

When we started this work our sole aim was to determine the $Ca^{2+}$ dependence of the $S_R$ recovery rate. We noted that $k_{tr}$ measurements indicate that populations of strongly bound force-generating cross-bridges develop force more quickly at high free $Ca^{2+}$ concentrations than at low (Brenner, 1988) and hypothesized that this effect might underlie a measurable increase in the rate of $S_R$ recovery. The experimental records summarized in Figs. 8 and 9 show this general postulate was indeed correct; the rate of $S_R$ recovery increased by a factor of ~2 when the pCa of the activating solution was reduced from 6.5 (minimal $Ca^{2+}$ activation) to 4.5 (saturating effect).

However, the magnitude of this increase was smaller than we had originally anticipated. The rate of $S_R$ recovery reached a minimum (0.73 $s^{-1}$) at pCa 6.2 and increased slightly with further reductions in the free $Ca^{2+}$ concentration (Fig. 9). This contrasts with the behavior observed in relaxed intact frog fibers where stiffness recovers much more slowly (0.1 $s^{-1}$ or less, Lännergren, 1971; Campbell and Lakie, 1998) even when the temperature (17°C, Lakie and Robson, 1988) exceeds that in the present experiments (15°C). We therefore conclude that the difference in stiffness recovery rates measured in chemically permeabilized mammalian fibers and relaxed intact frog fibers is not due solely to the level of $Ca^{2+}$ activation and must reflect other differences (mammalian versus amphibian, intact versus permeabilized, etc.) between the preparations.

As we noted above, our experiments started with a very simple objective. It was only once we had collected a consistent set of experimental data and started the analysis

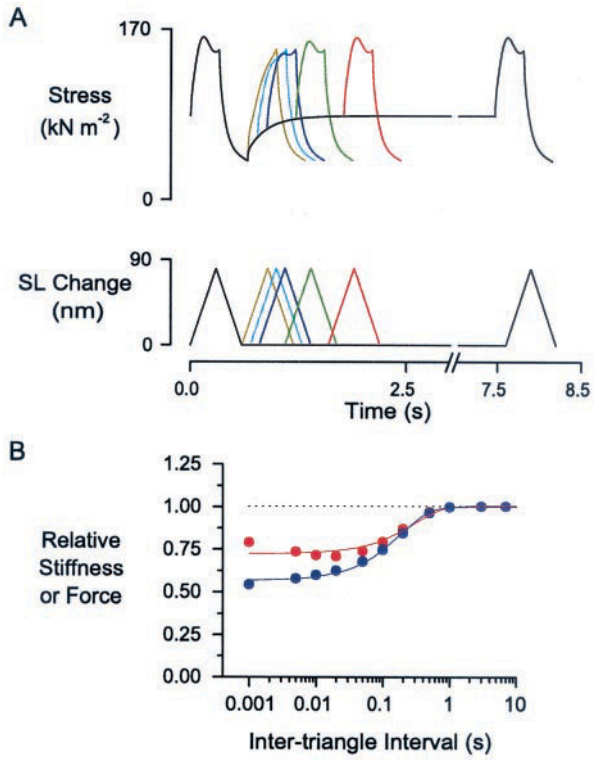


FIGURE 13 Simulated recovery time course. (*A*) Superimposed tension and sarcomere length records. Tension records simulated using the parameters described in Table 1 for trials (length change 0.03 $l_0$, velocity ± 0.10 $l_0$ $s^{-1}$) with intertriangle intervals ranging from 1 ms to 7 s. (*B*) Recovery time course. Symbols show the simulated relative stiffness ($S_R$, *red*) and relative tension ($T_R$, *blue*) values obtained for each intertriangle interval. Continuous lines are best fits of the form $y = [a - b \times \exp(-c \times \Delta t)]$ for each parameter. The simulated rates of $S_R$ and $T_R$ recovery were 3.31 and 5.36 $s^{-1}$, respectively. The simulation results may be compared with the analogous experimental records shown in Fig. 8 (*bottom right panel*).

that we realized that our experimental records contained a further layer of information. Whereas the $S_R$ and $T_R$ parameters, which formed the initial focus of our investigation describe the mechanical properties of the muscle fiber at the commencement of the second stretch, the $T_{E1}$ and $T_{E2}$ parameters (Fig. 6 *A*) describe the properties of the muscle during a sustained stretch and reveal an interesting $Ca^{2+}$ sensitivity.

At low levels of $Ca^{2+}$ activation, the $T_{E1}/T_{E2}$ ratio is markedly dependent on the duration of the intertriangle interval (Fig. 10), whereas at high levels of $Ca^{2+}$ activation the ratio is almost independent of recovery time. These results imply that the effects of prior movement on the muscle's mechanical properties can be quickly negated at high levels of $Ca^{2+}$ activation by stretching the muscle. It is important to realize that interfilamentary movement forms a crucial part of this rapid recovery. If the muscle is held at a constant sarcomere length, increasing the level of $Ca^{2+}$ activation speeds the recovery rates of the $S_R$ and $T_R$ parameters but does not eliminate the history-dependent reductions observed for short intertriangle intervals (Fig. 8).

We were intrigued by these observations, not only because to our knowledge they have not been previously described, but also because we thought that they might provide important new information on the underlying mechanism. The simulations presented in Figs. 12 and 13 were initiated in an effort to help us understand how cross-bridge populations would have to behave if they were to underlie the measured responses.

Although our model has shortcomings in its present form (our current simulations do not exactly reproduce the measured tension response at each level of $Ca^{2+}$ activation for example), this does not necessarily detract from the importance of the modeling process in our approach. Our simulations helped shape our interpretation of the experimental data and perhaps more importantly allowed us to develop two new hypotheses: 1) the rate of the force-generating power-stroke may increase with $Ca^{2+}$ activation and cross-bridge strain and 2) the parallel elastic component may be $Ca^{2+}$ sensitive, which cannot be deduced from purely mechanical measurements like our own without some sort of theoretical framework.

## Power stroke

If a population of cycling cross-bridges is perturbed by an imposed stretch, the population distributions for each attached state are displaced from their initial equilibrium profiles toward new steady-state profiles characteristic of the velocity of interfilamentary movement. The precise shape of the resulting force response depends on the details of the cross-bridge cycle, but the general features (an initial transient followed by a constant tension plateau) hold irrespective of the number of cross-bridge states.

Fig. 4 shows that in our experiments the measured force response remains approximately constant during the latter stages of the first stretch at every level of $Ca^{2+}$ activation. We think that this implies that the cross-bridge populations have adopted, or are at least approaching, the steady-state distributions produced during sustained movement. If this hypothesis is correct, the $T_{E1}$ parameter at each level of $Ca^{2+}$ activation is characteristic of the steady-state population distributions produced during movement.

In pCa 4.5 activating solution, $T_{E2}/T_{E1}$ is approximately unity, independent of the intertriangle interval (Fig. 10). This finding implies that the cross-bridge population distributions are equivalent at the end of the first and second stretches and (if $T_{E1}$ is the steady-state condition as argued above) that these are the equilibrium population distributions for the given interfilamentary velocity. At lower levels of $Ca^{2+}$ activation, $T_{E2}/T_{E1}$ is less than unity for short intertriangle intervals (Fig. 10), a finding that may be explained if the cross-bridge populations do not reach steady-state profiles during the second stretch. We are thus drawn

to the conclusion that cross-bridge redistribution occurs more quickly during stretch at high levels of $Ca^{2+}$ activation than at low levels.

If this is true, the rate at which cross-bridges progress through their cycling scheme must depend on both the level of activation and the mean cross-bridge strain. There are undoubtedly many ways in which this might be achieved, but we think that one of the simplest explanations is if the rate of the force-generating power-stroke ($k_2$ in our simulations, Fig. 11) increases with the intracellular free $Ca^{2+}$ concentration and the strain in the cross-bridge link. All other things being equal, cross-bridges would then enter the force-generating $A_2$ state more quickly at high than at low $Ca^{2+}$ concentrations, and the effect would be proportionally greater (resulting in a higher fraction of $A_2$ cross-bridges and thus more force) when the muscle is being stretched. This would explain, at least qualitatively, not only the $Ca^{2+}$ and history-dependence of the $T_{E2}/T_{E1}$ ratio (Fig. 10) but also the observed increases in $k_{tr}$ (Fig. 9) and the $T_{E1}/T_1$ ratio (Fig. 7 *D*) at high $Ca^{2+}$ concentrations.

The hypothesis does not explain why the maximal $T_{E2}/T_{E1}$ reduction occurs at an intermediate level of $Ca^{2+}$ activation (Fig. 10), but it is possible that this is not a simple kinetic effect. It may be more than coincidence that the maximal $T_{E2}/T_{E1}$ reduction occurs at the same level of $Ca^{2+}$ activation (pCa 6.2) as the minimal values of $k_{tr}$ and the $S_R$ and $T_R$ recovery rates (Fig. 9). One plausible explanation for the increase in each of these parameters at very low $Ca^{2+}$ concentrations is that the observed behavior reflects reduced cooperative interactions between thin filament regulatory units (Razumova et al., 2000). Such cooperative effects are important in regulating contractile activity (Fitzsimons et al., 2001) but were not considered in our current simulations.

We acknowledge that the evidence for our conjecture is not complete and that our hypothesis conflicts with some points of view. It has long been argued for example that the rate of the power-stroke step should be reduced during stretch (Julian et al., 1974; Lombardi and Piazzesi, 1990; Slawnych et al., 1994). Several workers have also probed the strain and $Ca^{2+}$ dependence of the power-stroke rate by measuring the effects of rapid changes in intracellular inorganic phosphate ($P_i$) concentration. Many of these experiments have yielded conflicting results, and it is difficult to reach firm conclusions. For example, Walker et al. (1992) found that the rate of force decline after photoliberation of $P_i$ in rabbit psoas fibers was enhanced at high $Ca^{2+}$ concentrations. This finding is consistent with our hypothesis that the power-stroke rate is increased at high levels of $Ca^{2+}$ activation but similar experiments conducted by Millar and Homsher (1990), and studies using rabbit psoas myofibrils and rapid solution switching techniques (Tesi et al., 2000) suggest that $Ca^{2+}$ concentration has a negligible effect. Homsher et al. (1997) investigated the strain dependence of the power-stroke rate by liberating caged $P_i$ during controlled length changes. They concluded that the rate of the force-generating cross-bridge transition was increased when the muscle was allowed to shorten but did not decrease when the muscle was forcibly lengthened. Whether these experimental results would apply directly to the rat soleus muscle fibers used in our own experiments is unclear. Homsher and Millar (1993) point out that the force transient induced by phosphate release is much slower in rabbit soleus fibers than in rabbit psoas fibers and is highly temperature dependent.

## Parallel component

When we started our simulations, we thought that we might be able to omit the parallel component from our model (equivalent to setting $\sigma_P$ equal to zero in Table 1) because the measured tension responses did not rise during the latter stages of the first stretch (Fig. 4) and therefore seemed to be qualitatively consistent with the general transient/plateau response expected from cycling cross-bridges. Our initial calculations showed that this was indeed the case if we confined our simulations to the lengthening phase of the first triangular movement. When the model parameters were chosen appropriately, the simulated cross-bridge tension response was almost indistinguishable from the corresponding experimental record during the first stretch.

However, these parameters did not simultaneously produce a satisfactory fit to the second stretch response, and despite intensive efforts we were unable to find cross-bridge cycling parameters that matched the history dependence of the muscle's mechanical properties. If cross-bridges cycled sufficiently quickly to maintain the elevated tension plateau during the first stretch, tension always rose too sharply during the initial phase of the second stretch for short intertriangle intervals and overshot the steady-state plateau.

Although we do not rule out the possibility that our cross-bridge cycling scheme (Fig. 11) could be adapted (perhaps by including cooperative effects (Razumova et al., 2000), additional cross-bridge states (Lombardi and Piazzesi, 1990; Getz et al., 1998), and/or velocity-dependent rate constants (Campbell and Lakie, 1998)) we have been unable to obtain satisfactory fits to the full experimental records to date without including a parallel elastic element in our simulations. The parallel element (Eq. A1 in Campbell and Moss, 2000) is mathematically identical to the one we postulated for rabbit psoas fibers and produces a force that rises monotonically with sarcomere length, producing proportionately more force the further the muscle is stretched. Its contribution to the simulated response is shown by the blue line in Fig. 12.

As one might expect from the preceding arguments, the magnitude of the parallel elastic force in our current simulations is less than that postulated for rabbit psoas fibers. The elastic tension at a half-sarcomere extension of 40 nm (the maximal length change used in the current experi-

ments) is 43.4 kN $m^{-2}$ (Table 1); the corresponding value for our simulations of rabbit psoas fibers was 54.3 kN $m^{-2}$ (Campbell and Moss, 2000). This difference probably reflects the distinct titin isoforms expressed in each fiber type. Titin molecules in rabbit soleus muscles (molecular mass = 3.35 MDa) are under less strain at a given sarcomere length than in psoas muscles (3.70 MDa) because their I-band segments have longer PEVK and proximal tandem immunoglobulin domains (Freiburg et al., 2000). Similar conclusions would be expected for the rat soleus muscles used in our present experiments.

This conjecture is supported by our experimental results. In the present experiments using rat soleus fibers, resting tension in pCa 9.0 solution at a sarcomere length of 2.57 ± 0.02 $\mu$m ($n$ = 5 preparations) was 1.25 ± 0.26 kN $m^{-2}$. Stiffness was 0.19 ± 0.07 MN $m^{-2}$ (Young's Modulus). The corresponding results for rabbit psoas fibers at a sarcomere length of 2.59 ± 0.03 $\mu$m ($n$ = 5 preparations) were substantially greater. Resting tension was 6.6 ± 1.1 kN $m^{-2}$ and stiffness equaled 0.33 ± 0.04 MN $m^{-2}$ (Campbell and Moss, 2000). Although this analysis compares the relaxed properties of fibers isolated from rats and rabbits, similar differences in resting tension have also been reported for different fiber types from rabbit (Horowits, 1992; Freiburg et al., 2000).

We would like to draw attention to three additional points. First, although variations in titin isoform expression probably account for the different passive mechanical properties of soleus and psoas fibers, different titin isoforms seem unlikely to underlie the enhanced stability of the striation pattern observed in the present experiments. Titin is more compliant in soleus than in psoas fibers and would provide less restoring force to center A-bands within the sarcomere (Horowits, 1992).

Second, a slight discontinuity in the pCa 9.0 tension response was normally observed when the muscle was stretched after a period at fixed length (Fig. 5). The change in stiffness at the discontinuity (if present) is very small in our experiments and, given recent controversy regarding the thixotropic properties of relaxed skeletal muscles (Mutungi and Ranatunga, 2000), is probably subject to a number of different interpretations. It may reflect titin filaments (and their history dependence (Kellermayer et al., 2001, Minajeva et al., 2001)) or a viscous drag between the myofilaments (Bagni et al., 1995; Mutungi and Ranatunga, 1996). We however were struck by the fact that the discontinuity occurs at almost exactly the same sarcomere length as the (much more dramatic) discontinuity observed in $Ca^{2+}$-activated fibers (Fig. 5). Therefore, it seems to us that the underlying mechanism may be the same in both cases and that the discontinuity observed in pCa 9.0 solution may reflect the forcible detachment of a very small number of residual cross-bridges bound to the thin filament in pCa 9.0 solution.

Third, our experimental records indicate that the stiffness of the parallel elastic component may increase with the level of $Ca^{2+}$ activation. Although we can only estimate the parallel elastic force in contracting fibers from the results of our simulations, the best-fit parameters (Table 1) indicate that the initial tension ($\sigma_P$) and parallel stiffness (approximated by linear regression) are greater in pCa 4.5 solution by factors of 8 and 3, respectively, than the corresponding values measured in pCa 9.0 solution. We noted a similar effect in our previous experiments with rabbit psoas fibers (Campbell and Moss, 2000).

The underlying cause for the apparent $Ca^{2+}$ sensitivity of the parallel elastic component remains uncertain. We think that it is unlikely that the effect can be attributed to series compliance, which as far as we can tell is minimal in our preparations. One good indication of this is that the fiber length change required to produce a fixed increase in measured sarcomere length remained approximately constant as the level of $Ca^{2+}$ activation was raised from minimum to saturating values (Fig. 4). Neither do we think that the apparent stiffening of the parallel component is due to the development of sarcomere length inhomogeneities (Morgan, 1990). The striation patterns in our preparations were remarkably stable as demonstrated by the fact that we were able to maintain sarcomere length control for extended periods of time (more than 11 min at maximal $Ca^{2+}$ activation in some cases). An intriguing possibility is that the stiffness of titin filaments varies with the intracellular free $Ca^{2+}$ concentration, perhaps as a result of a conformational change due to $Ca^{2+}$ binding (Tatsumi et al., 1997). Stuyvers et al. (1998) have also suggested that titin stiffness may be $Ca^{2+}$ sensitive, although their experiments used cardiac muscles (which may possess a different titin $Ca^{2+}$ sensitivity than skeletal muscles) and indicated that titin stiffness decreased (rather than increased) with rising $Ca^{2+}$ concentrations.

We are not the first to suggest that skeletal muscles may possess an elastic component with a stiffness, which increases with the free $Ca^{2+}$ concentration and yet which is not attributable to cycling cross-bridges. Bagni et al. (1994) described a "static stiffness" in intact frog fibers, which showed no signs of "give" during long stretches, was unaffected by 2,3-butanedione-2-monoxime, and which increased with a time course similar to the intracellular free $Ca^{2+}$ concentration after a single electrical stimulus. Bagni et al. were unable to identify the responsible structure(s) (see also Cecchi, 2000), but the properties of their static stiffness seem compatible with the parallel elastic component postulated in our simulations.

## Sarcomere length control

Our experimental records show that it is possible to maintain sarcomere length control in permeabilized mammalian fibers for extended periods. In several of our experiments,

single muscle fibers were activated in pCa solutions ranging from 6.5 to 4.5 for a total of ~90 min and stretched ~500 times without substantial changes in their appearance or mechanical behavior. This is a substantial improvement on previous experiments using permeabilized rabbit psoas fibers (Getz et al., 1998; Campbell and Moss, 2000). Although we do not know precisely why the striation pattern in the soleus muscle fibers is maintained during these prolonged activations, one possible explanation is that fast and slow-twitch fibers express different amounts of intermediate filament proteins (Price, 1991). These proteins link myofibrils transversely within each fiber, and there is increasing evidence that they may play an important role in maintaining the three-dimensional integrity of the sarcomeric repeat (Boriek et al., 2001).

We thank a number of colleagues for their contributions to this work. M. Greaser (Muscle Biology Laboratory, UW-Madison), J.M. Ervasti (Dept. of Physiology, UW-Madison), and J.W. Walker (Dept. of Physiology, UW-Madison) advised us on the properties of titin molecules, lattice filament systems, and the activation dependence of cross-bridge cycling rate constants, respectively. D.P. Fitzsimons and J.R. Patel (from our laboratory) helped with some of the initial experiments and provided valued advice and encouragement throughout the course of this work.

This work was supported by grants from the American Heart Association and the National Institutes of Health (AHA 9920545Z to K.S.C. and National Institutes of Health HL47053 to R.L.M.). K.S.C. is a Postdoctoral Fellow of the Northland Affiliate of the American Heart Association.

## REFERENCES

Bagni, M. A., G. Cecchi, F. Colomo, and P. Garzella. 1994. Development of stiffness precedes crossbridge attachment during the early tension rise in single frog muscle fibres. *J. Physiol. (Lond.).* 481:273–278.

Bagni, M. A., G. Cecchi, F. Colomo, and P. Garzella. 1995. Absence of mechanical evidence for attached weakly binding crossbridges in frog relaxed muscle fibres. *J. Physiol. (Lond.).* 482:391–400.

Boriek, A. M., Y. Capetanaki, W. Hwang, T. Officer, M. Badshah, J. Rodarte, and J. G. Tidball. 2001. Desmin integrates the three-dimensional mechanical properties of muscles. *Am. J. Physiol.* 280: C46–C52.

Brenner, B. 1988. Effect of $Ca^{2+}$ on cross-bridge turnover kinetics in skinned single rabbit psoas fibers: implications for regulation of muscle contraction. *Proc. Natl. Acad. Sci. U. S. A.* 85:3265–3269.

Campbell, K. S., and M. Lakie. 1998. A cross-bridge mechanism can explain the thixotropic short-range elastic component of relaxed frog skeletal muscle. *J. Physiol. (Lond.).* 510.3:941–962.

Campbell, K. S., and R. L. Moss. 2000. A thixotropic effect in contracting rabbit psoas muscle: prior movement reduces the initial tension response to stretch. *J. Physiol. (Lond.).* 525.2:531–548.

Campbell, K. S., and R. L. Moss. 2001. History dependent stiffness in slow twitch skeletal muscle. *Biophys. J.* 80:273A.

Cecchi, G. 2000. Do cross-bridges contribute to the tension during stretch of passive muscle? *J. Muscle. Res. Cell. Motil.* 21:99.

Denny-Brown, D. 1929. On the nature of postural reflexes. *Proc. R. Soc. Lond. B. Biol. Sci.* 104:252–301.

Edman, K. A. P. 1999. The force bearing capacity of frog muscle fibers during stretch: its relation to sarcomere length and fibre width. *J. Physiol. (Lond.).* 519:515–526.

Edman, K. A. P., G. Elzinga, and M. I. M. Noble. 1978. Enhancement of mechanical performance by stretch during tetanic contractions of vertebrate skeletal muscle fibers. *J. Physiol. (Lond.).* 281:139–155.

Fabiato, A. 1988. Computer programs for calculating total from specified free or free from specified total ionic concentrations in aqueous solutions containing multiple metals and ligands. *Methods Enzymol.* 157: 378–417.

Fitzsimons, D. P., J. R. Patel, K. S. Campbell, and R. L. Moss. 2001. Cooperative mechanisms in the activation dependence of the rate of force development in rabbit skinned skeletal muscle fibers. *J. Gen. Physiol.* 117:113–148.

Flitney, F. W., and D. G. Hirst. 1978. Crossbridge detachment and sarcomere 'give' during stretch of active frog's muscle. *J. Physiol. (Lond.).* 276:449–465.

Freiburg, A., K. Trombitas, W. Hell, O. Cazorla, F. Fougerousse, T. Centner, B. Kolmerer, C. Witt, J. S. Beckmann, C. C. Gregorio, H. Granzier, and S. Labeit. 2000. Series of exon-skipping events in the elastic spring region of titin as the structural basis for myofibrillar elastic diversity. *Circ. Res.* 86:1114–1121.

Getz, E. B., R. Cooke, and S. L. Lehman. 1998. Phase transition in force during ramp stretches of skeletal muscle. *Biophys. J.* 75:2971–2983.

Godt, R. E., and B. D. Lindley. 1982. Influence of temperature upon contractile activation and isometric force production in mechanically skinned muscle fibers of the frog. *J. Gen. Physiol.* 80:279–297.

Gordon, A. M., E. Homsher, and M. Regnier. 2000. Regulation of contraction in striated muscle. *Physiol. Rev.* 80.2:853–924.

Herbst, M. 1976. Studies on the relation between latency relaxation and resting cross-bridges of frog skeletal muscle. *Pflügers Arch.* 364:71–76.

Hill, D. K. 1968. Tension due to interaction between the sliding filaments in resting striated muscle: the effect of stimulation. *J. Physiol. (Lond.).* 199:637–684.

Homsher, E., J. Lacktis, and M. Regnier. 1997. Strain-dependent modulation of phosphate transients in rabbit skeletal muscle fibers. *Biophys. J.* 72:1780–1791.

Homsher, E., and N. Millar. 1993. Kinetics of force generation and $P_i$ release in rabbit soleus muscle fibers. *In* Mechanism of Myofilament Sliding in Muscle Contraction. H. Sugi and G. H. Pollack, editors. Plenum Press, New York. 495–503.

Horowits, R. 1992. Passive force generation and titin isoforms in mammalian skeletal muscle. *Biophys. J.* 61:392–398.

Julian, F. J., K. R. Sollins, and M. R. Sollins. 1974. A model for the transient and steady-state mechanical behavior of contracting muscle. *Biophys. J.* 14:546–562.

Kellermayer, M. S. Z., S. B. Smith, C. Bustamante, and H. L. Granzier. 2001. Mechanical fatigue in repetitively stretched single molecules of titin. *Biophys. J.* 80:852–863.

Lakie, M., and L. G. Robson. 1988. Thixotropy: stiffness recovery rate in relaxed frog muscle. *Q. J. Exp. Physiol.* 73:237–239.

Lakie, M., and L. G. Robson. 1990. Thixotropy in frog single muscle fibres. *Exp. Physiol.* 75:123–125.

Lännergren, J. 1971. The effect of low-level activation on the mechanical properties of isolated frog muscle fibers. *J. Gen. Physiol.* 58:145–162.

Lombardi, V., and G. Piazzesi. 1990. The contractile response during steady lengthening of stimulated frog muscle fibres. *J. Physiol. (Lond.).* 431:141–171.

Metzger, J. M., and R. L. Moss. 1990. Calcium-sensitive cross-bridge transitions in mammalian fast and slow skeletal muscle fibres. *Science.* 247:1088–1090.

Millar, N. C., and E. Homsher. 1990. The effect of phosphate and calcium on force generation in glycerinated rabbit skeletal muscle fibers. *J. Biol. Chem.* 265:20234–20240.

Minajeva, A. V. E., M. Kulke, J. M. Fernandez, and W. A. Linke. 2001. Unfolding of titin domains explains the viscoelastic behavior of skeletal myofibrils. *Biophys. J.* 80:1442–1451.

Morgan, D. L. 1990. New insights into the behavior of muscle during active lengthening. *Biophys. J.* 57:209–221.

Mutungi, G., and K. W. Ranatunga. 1996. The viscous, viscoelastic and elastic characteristics of resting fast and slow mammalian (rat) muscle fibres. *J. Physiol. (Lond.).* 496.3:827–836.

Mutungi, G., and K. W. Ranatunga. 2000. Do cross-bridges contribute to the tension response during stretch of passive muscle: a response. *J. Muscle. Res. Cell. Motil.* 21:301–302.

Press, W. H., S. A. Teukolsky, W. T. Vetterling, and B. P. Flannery. 1992. Numerical Recipes in C: The Art of Scientific Computing. Cambridge University Press, Cambridge.

Price, M. G. 1991. Striated muscle endosarcomeric and exosarcomeric lattices. *Adv. Struct. Biol.* 1:175–207.

Proske, U., and D. L. Morgan. 1999. Do cross-bridges contribute to the tension during stretch of passive muscle? *J. Muscle. Res. Cell. Motil.* 20:433–442.

Razumova, M. V., A. E. Bukatina, and K. B. Campbell. 2000. Different myofilament nearest-neighbour interactions have distinctive effects on contractile behavior. *Biophys. J.* 78:3120–3137.

Slawnych, M. P., C. Y. Seow, A. F. Huxley, and L. E. Ford. 1994. A program for developing a comprehensive mathematical description of the crossbridge cycle of muscle. *Biophys. J.* 67:1669–1677.

Stienen, G. J., P. G. Versteeg, Z. Papp, and G. Elzinga. 1992. Mechanical properties of skinned rabbit psoas and soleus muscle fibres during lengthening: effects of phosphate and $Ca^{2+}$. *J. Physiol. (Lond.)*. 451: 503–523.

Stuyvers, B. D., Miura, M., Jin, J.-P. and ter Keurs, H. E. D. J. 1998. $Ca^{2+}$-dependence of diastolic properties of cardiac sarcomeres: involvement of titin. *Prog. Biophys. Mol. Biol.* 69:425–433.

Tatsumi, R., K.-I. Shimada, and A. Hattori. 1997. Fluorescence detection of calcium-binding proteins with Quinoline Ca-indicator Quin2. *Anal. Biochem.* 254:126–131.

Tesi, C., F. Colomo, S. Nencini, N. Piroddi, and C. Poggesi. 2000. The effect of inorganic phosphate on force generation in single myofibrils from rabbit skeletal muscle. *Biophys. J.* 78:3081–3092.

Walker, J. W., Z. Lu, and R. L. Moss. 1992. Effects of $Ca^{2+}$ on the kinetics of phosphate release in skeletal muscle. *J. Biol. Chem.* 267:2459–2466.